03,08

Electronic band structure and thermoelectric properties of $SrTiO_3$, $BaTiO_3$ and $CaTiO_3$: *ab initio* approach

© V.P. Zhukov[1], E.V. Chulkov[2,3]

[1] Institute of Solid State Chemistry, Russian Academy of Sciences, Ural Branch, Yekaterinburg, Russia
[2] St. Petersburg State University, St. Petersburg, Russia
[3] Dpto. de Polímeros y Materiales Avanzados: Física, Química y Tecnología, Facultad de Ciencias Químicas, Aptdo. 1072, 20018, San Sebastián, España

E-mail: Zhukov@ihim.uran.ru

Received May 20, 2022
Revised May 20, 2022
Accepted May 22, 2022

The calculations of Seebeck's coefficient, conductivity and power functions for the electron-doped $SrTiO_3$, $BaTiO_3$ and $CaTiO_3$ compounds have been performed depending on temperature and current carrier concentration by employing ab initio method based on the electron density functional theory, on the Frohlich's approach for the electron-phonon interaction and on the theory of Boltzmann–Onsager for the thermoelectric properties. The calculated Seebeck's coefficient and conductivity correspond to experimental data. It is shown that for $SrTiO_3$ and $BaTiO_3$ the dependencies of power functions on the carrier concentration have maxima in the range of $(200-250)\cdot 10^{19}\,\mathrm{cm}^{-3}$ at any temperature, while for $CaTiO_3$ the maxima are typical only at temperatures below 500 K. The temperature dependencies of the power function also confirm that such carrier concentration range is favorable for achieving high values of the $SrTiO_3$ figure of merit, while the maximally possible carrier concentration is necessary for optimal $CaTiO_3$ figure of merit.

Keywords: Ca, Sr, Ba titanates, PAW method, electronic structure, thermoelectric properties.

DOI: 10.21883/PSS.2022.12.54377.383

1. Introduction

The search for materials for efficient thermoelectric converters is one of the current directions of modern physics and chemistry [1]. The efficiency of a thermoelectric generator is defined as [1]:

$$\eta = \frac{T_h - T_c}{T_h}\,\frac{\sqrt{1+ZT_m}-1}{\sqrt{1+ZT_m}+T_c/T_h}, \qquad (1)$$

where T_h, T_c are temperatures, respectively, of the hot and cold parts of the generator, T_m — the average temperature of the generator, and the temperature-dependent dimensionless value ZT, the so-called figure of merit of the material, is defined as

$$ZT = \frac{S^2\sigma}{k}\,T. \qquad (2)$$

Here S is Seebeck coefficient, σ is electrical conductivity, k is thermal conductivity of the material. In search for materials with maximum values of ZT, a large number of works were carried out on the synthesis and study of the characteristics of chemical compounds with a diverse structure and morphology: single crystals, polycrystals, films, nanostructures, etc. In particular, it was shown that effective thermoelectrics can be synthesized on the basis of compounds $ATiO_3$ with a perovskite structure, where $A = \mathrm{Sr, Ba}$ or Ca, doped with elements of the third or fifth groups. For some of them, as, for example, for compositions close to $Sr_{0.5}Ca_{0.5}TiO_3$, high values of ZT, up to 0.4 are observed. In a number of studies, dependences of ZT, S, σ and k on the temperature and concentration of carriers were obtained. An overview of experimental data on thermo-electric characteristics (TEC) of $SrTiO_3$, $BaTiO_3$ and $CaTiO_3$ is available in articles [2] on phase diagrams, in articles [3,4] on methods of obtaining thermoelectrics, their structure, conductivity, thermal conductivity and ZT values. Most fully TECs have been studied for doped $SrTiO_3$ [5–18]. The properties of doped $BaTiO_3$ have been studied in Refs. [19–24], and there are only a few papers on the synthesis and TEC of $CaTiO_3$ [25–27]. A number of information about the composition, structure of samples and their TEC is given in Table 1.

Here we limit ourselves to data on $SrTiO_3$ samples doped with La or Nb, which indicate a significant dependence of the TEC on the morphology of the samples, as well as the presence of contradictions in the experimental data. It follows from the table that the values of the Seebeck coefficient, depending on the composition and morphology of the sample, vary from -80 to $-420\,\mu$V/K, which indicates the electronic nature of the electrical conductivity, and the conductivity values vary very widely. Comparing the work data [5] and [6] or [14] and [18], we see that the conductivity values do not correlate with the electron con-

Table 1. Experimental thermoelectric characteristics of a number of samples of strontium titanate doped with lanthanum or niobium

Source	Composition	Structure of	Concentration media, $1/cm^3$	Seebeck coefficient at 300 K, $\mu V/K$	Conductivity at 300 K, $S \cdot cm^{-1}$ (4-pin method)
[5]	$Sr_{1-x}La_xTiO_3$ $0 \le x \le 0.1$	Single crystal	$(0.005-0.11) \cdot 10^{20}$	$(-380)-(-80)$	$0.52 \cdot 106$ $(x = 0.02)$, $3.57 \cdot 10^6$ $(x = 0.11)$
[11]	$Sr_{0.92}La_{0.09}TiO_{3-\delta}$, $\delta = 0.02-0.06$	Polycrystal	–	$(-120)-(-90)$	1000–4000
[16]	$Sr_{0.85}La_{0.15}TiO_3$	Film	$(4-12) \cdot 10^{20}$	$(-250)-(-140)$	–
[6]	$Sr_{1-x}La_xTiO_3$	Single crystal	$(0.5, 6.8) \cdot 10^{20}$	$(-420)-(-150)$	54, 1000
[10]	$SrTi_{0.85}Nb_{0.15}O_3$	Powder	$2.5 \cdot 10^{21}$	-390	–
[14]	$SrTi_{1-x}Nb_xO_3$, $x = 0-0.37$	Film	$(0-3.3) \cdot 10^{21}$	$(-175)-(-125)$	$8.33 \cdot 10^6$ $(x = 0.12, 0.20)$
[18]	$SrTi_{1-x}Nb_xO_3$, $x = 0.02-0.06$	Powder		$(-215)-(-140)$	100–700

centration values, i.e., apparently, the electrical conductivity depends not only on the electronic structure, but also on the presence of defects, and from the microstructure of the samples, particularly, on the resistance at the boundaries of microcrystals.

As for $BaTiO_3$, there is only one work [20] in which the TEC are considered in the temperature range below 400 K. In a number of other studies [18,20,22] attention is mainly paid to the ferroelectric properties of phases based on $BaTiO_3$. The TEC values published in these papers are limited by temperatures below 400 K, and they have a very irregular appearance due to the presence of a number of phase transitions between structures that are not fully studied. There is little experimental information about phases based on $CaTiO_3$: only in the study [27] there is information about the Seebeck coefficient and conductivity in $CaTiO_3$ containing oxygen vacancies and doped with lanthanum.

In general, the existing contradictions in the experimental data on TEC, and the deficite of accumulated data do not allow us to identify patterns of changes in the properties of doped phases depending on their electronic structure, which is largely responsible for the values, included in the definition of ZT. The value $P = S^2\sigma$, so-called power function, is of special significance. Since the concentration of doping elements is usually significantly lower than the concentration of the main elements in the sublattices, it can be assumed that at a fixed temperature, depending on the concentration of dopants, the thermal conductivity changes slightly. It follows that the dependence of ZT on the concentration of dopants is determined mainly by the power function, hence its estimation can therefore serve as a tool of finding optimal concentrations of dopants.

The first-principle calculations of electronic structure and the properties of compounds can provide some help in this direction. An overview of the performed studies of this type is available in [2], and here we will indicate only those works in which the studies were brought to the calculations of conductivity, Seebeck coefficient, thermal conductivity and ZT value. For phases based on $SrTiO_3$, such studies were carried out in [11,28,29], for compounds based on $BaTiO_3$ and $CaTiO_3$ — in [26]. The researches were performed based on the Boltzmann theory, Onsager theory and using the methods of TEC calculations. The disadvantage of the approaches used in these works was the use of a fixed electron relaxation time approximation, i.e., independent on the electron energy and wave vector. This does not allow us to obtain sufficiently accurate values of the Seebeck coefficient, and the conductivity σ is obtained only in the form of a combination σ/τ. In addition, electron relaxation due to interaction with defects is not taken into account. Therefore, for the theoretical analysis of TEC changes depending on the thermoelectric material's composition, and much more for predicting the properties of new compositions, it is necessary to use more advanced calculation methods „from the first principles“, for example, the methods developed in the studies [30–32]. In this regard, we have undertaken a theoretical study of the electronic band structure and the TEC of electronically doped $SrTiO_3$, $BaTiO_3$ and $CaTiO_3$ using the recently developed approach „from the first principles“ [32], which takes into account all the basic mechanisms of conduction electrons scattering. Since there are no theoretical estimates of the power function dependencies on the carrier concentration in the literature, we performed the corresponding calculations. Based on the calculations, the doping level was also estimated.

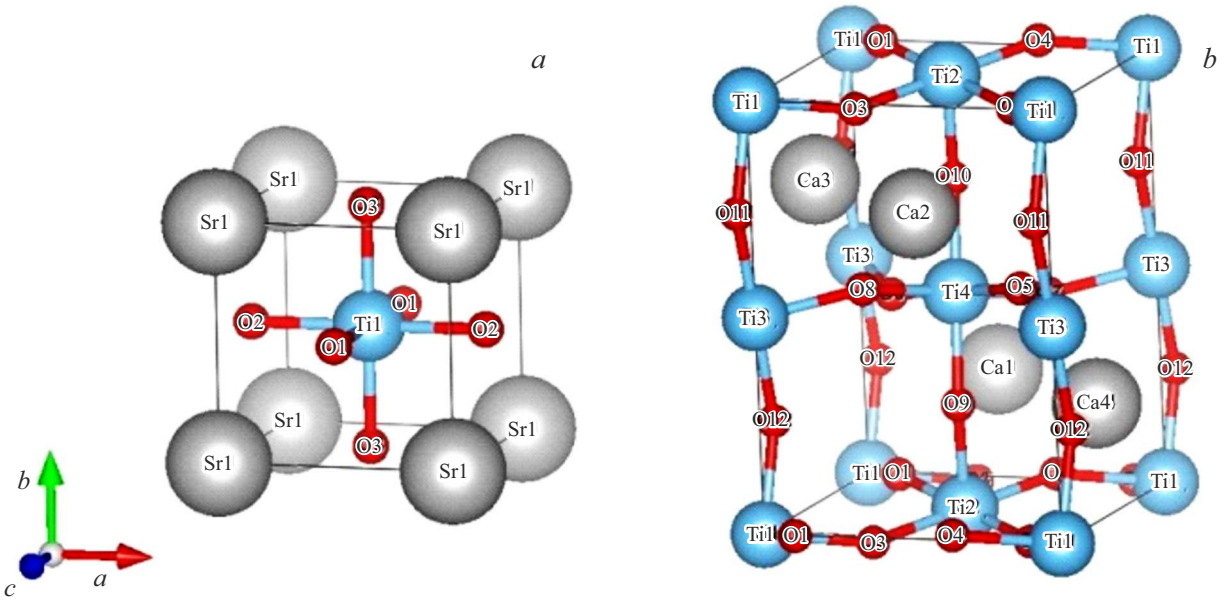

Figure 1. Unit cells $SrTiO_3$ or $BaTiO_3$ (a) and $CaTiO_3$ (b).

2. Method for calculating the band structure and thermoelectric characteristics

The unit cells of $SrTiO_3$, $BaTiO_3$ and $CaTiO_3$ are shown in Fig. 1. Strontium titanate crystallizes in a simple cubic structure of the perovskite type, Fig. 1, *a*. Similarly, barium titanate has a cubic structure of the perovskite type at temperatures above 130°C. As for calcium titanate, at a temperature from 300 to 1470 K it has an orthorhombic structure of the symmetry type P_{nma} [33], Fig. 1, *b*, with a doubled period *b* due to the zigzag articulation along this direction in the chain Ti1−O12−Ti3−O11−Ti1 (the so-called tilting). Calculations of the electronic band structure, which served as the basis for calculating the TEC, were performed by the pseudopotential projector augmented wave method theory (PAW) of the electron density functional, implemented in the VASP [34] software package. Pseudopotentials supplied with the program were used, based on the Generalized Gradient Approximation (GGA) of the exchange-correlation interaction. The decomposition of pseudo-wave functions was carried out on the basis of plane waves with energy up to 300 eV. Calculations were performed for 125 wave vectors uniformly distributed in the irreducible part of the Brillouin zone.

Since the TEC calculations by the method described in [32] require the calculation of elastic constants and deformation potentials of electronic states, in all cases the search was carried out for the minimum of the total energy of compounds, i.e. the relaxation of the crystal structure was modeled in accordance with the forces acting on atoms, as per the method described in [34]. The iterative process of searching for the minimum of the total energy was considered complete when its variations did not exceed 10^{-4} eV, and the residual forces acting on the atoms were no more than 0.005 eV/Å. Some characteristics of the relaxed crystal structure are compared with experimental data in Table 2.

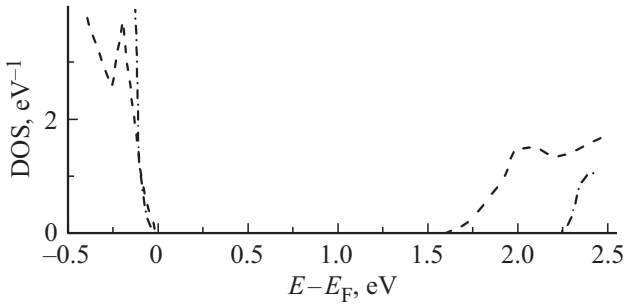

Figure 2. Densities of electronic states near the band gap for $SrTiO_3$, $BaTiO_3$ (dashed line), $CaTiO_3$ (dash-and-dot line). The top of the valence band is taken as zero.

It can be seen that the structure obtained as a result of relaxation, both in terms of lattice periods and angles between bonds, corresponds well to experimental data. A noteworthy factor is that the relaxed structure correctly reproduces the zigzag nature of the chain of bonds Ti−O12−Ti3−O11−Ti1 with a small deviation of the angle Ti−O−Ti from the experimental value. The densities of electronic states obtained for relaxed structures near the band gap are shown in Fig. 2.

As is the case when using the exchange-correlation GGA potential, the band gap width turns out to be underestimated in comparison with experimental data. This error was eliminated by using the so-called „scissor operator“, which

Table 2. Calculated (after relaxation) and experimental (in brackets) characteristics of the crystal structure $SrTiO_3$, $BaTiO_3$, $CaTiO_3$

Characteristic	$SrTiO_3$	$BaTiO_3$	$CaTiO_3$
Lattice periods a, b, c, Å	3.9218 (3.9050)	4.0098 (3.9920)	5.4735, 7.6493, 5.3760 (5.4289, 7.6389, 5.3779)
Distance TiO, Å	1.9609 (1.9525)	2.0049 (1.9960)	1.9736, 1.9686, 1.9632 (2.0018, 1.9857, 1.9918)
Angle Ti−O−Ti (along b), °	180 (180)	180 (180)	153.85 (147.11)
Angle Ti−O−Ti (in plane ac), °	180 (180)	180 (180)	153.85 (146.74)

shifts the states of the conduction band to match the band gap width with the experimental value, i.e. 3.2 eV for $SrTiO_3$, $BaTiO_3$ and 3.5 eV for $CaTiO_3$. We note that the band gap for $CaTiO_3$ is noticeably larger than for $SrTiO_3$, $BaTiO_3$, which, as will be shown below, leads to noticeable differences in the TEC values.

The appearance of vacancies in the oxygen sublattice, the doping of the Ti sublattice with pentavalent elements or the Ca, Sr and Ba sublattices with trivalent elements leads to the appearance of conductivity due to a shift into the conduction band of the Fermi level, which at typical doping levels $\sim 10^{19}-10^{21}\,\mathrm{cm}^{-3}$ is located above the bottom of this zone at 0.1−0.2 eV. The correct choice of the concentration of current carriers is essential in TEC calculations. With a known level of doping x in $ATi_{1-x}M_xO_3$, where $A =$ Ca, Sr, Ba, $M =$ Nb, Ta, basing on the dependence of the integrated density of states on energy, it is possible to find the dependences of the carrier concentration on x. However, we preferentially used similar dependences obtained in experimental studies by Hall measurements. In high-temperature synthesis, conduction electrons actually appear not only due to the presence of doping elements, but also due to the appearance of oxygen vacancies and, possibly, nitrogen or carbon impurities, therefore, Hall coefficient measurements allow obtaining more reliable values of carrier concentrations.

The main point in TEC calculations according to the methodology we use [32] is the choice of electron scattering mechanisms taken into account, which can be scattering by polar optical phonons (POP), scattering by acoustic phonons (SAP), scattering by local defects (SLD), piezoelectric scattering by acoustic phonons (PSAP). The PSAPh mechanism for perovskites is obviously ineffective, since it is valid only for non-isomorphic crystals [35]. In order to identify the most important scattering mechanisms, we performed calculations of the Seebeck coefficient and conductivity for $SrTiO_3$ taking into account 1) only the POPh mechanism, 2) scattering of POP and SAP types, as well as 3) POP, SAP and SLD scattering. The obtained conductivity data are shown in Fig. 3. It can be seen that the results of the POP mechanism differ slightly from the results of other more complex calculations only at room temperature, whereas at temperatures above 400 K for the three calculation modes they are almost identical. Similarly, the results for the values of the Seebeck coefficient are almost the same. That is, the main mechanism responsible for the scattering of conduction electrons seems to be Fröhlich scattering on polar optical phonons. The comparison of the results obtained with the experiments given below, taking into account the POP mechanism, confirms the dominant role of this mechanism.

The accuracy of TEC calculation of $SrTiO_3$ is characterized by Figs. 4, 5, on which we present a comparison of the calculated ones with experimental data on doped perovskites $SrTi_{1-x}Nb_xO_3$ [18].

It follows that the calculated conductivity data at three carrier concentrations taken from [18] are significantly higher in accuracy than the results in [36] obtained earlier by the PERTURBO method [30]. At concentrations $4.97 \cdot 10^{19}$, $5.98 \cdot 10^{19}\,\mathrm{cm}^{-3}$ both calculated and experimental temperature dependences of σ correspond to metallic conductivity. At a concentration $7.98 \cdot 10^{19}$, electronic conductivity is also observed in the experiment at $T > 470$ K, however, at a lower temperature, the conductivity has a semicon-

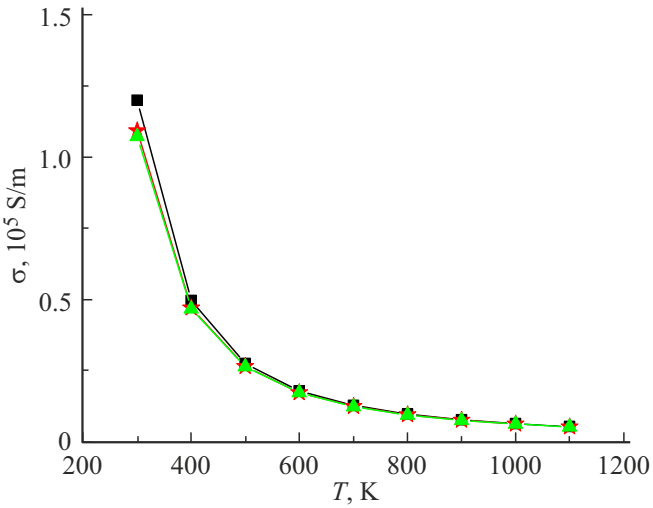

Figure 3. The results of conductivity calculations of $SrTiO_3$ in the approximations of POP (squares), POP + SAP (asterisks) and POP + SAP + SLD (triangles).

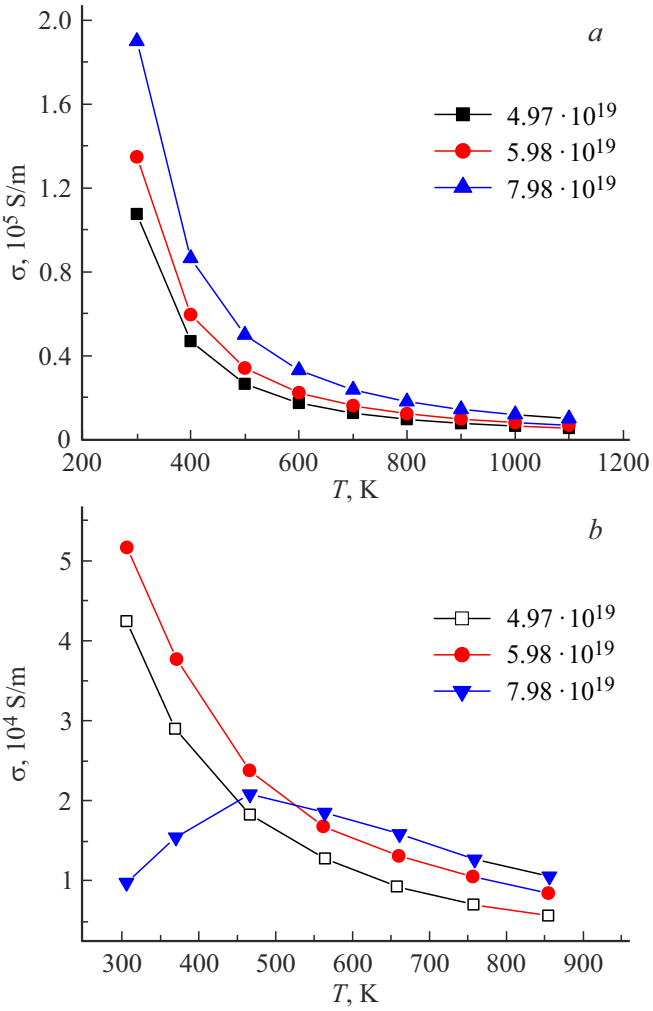

Figure 4. Theoretical (a) and experimental [18] (b) conductivity data σ of doped $SrTiO_3$.

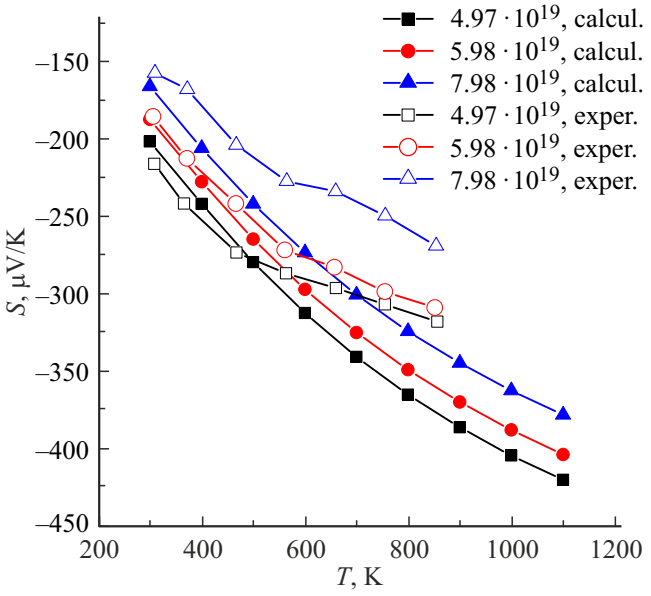

Figure 5. Calculated and experimental [18] values of the Seebeck coefficient for doped $SrTiO_3$.

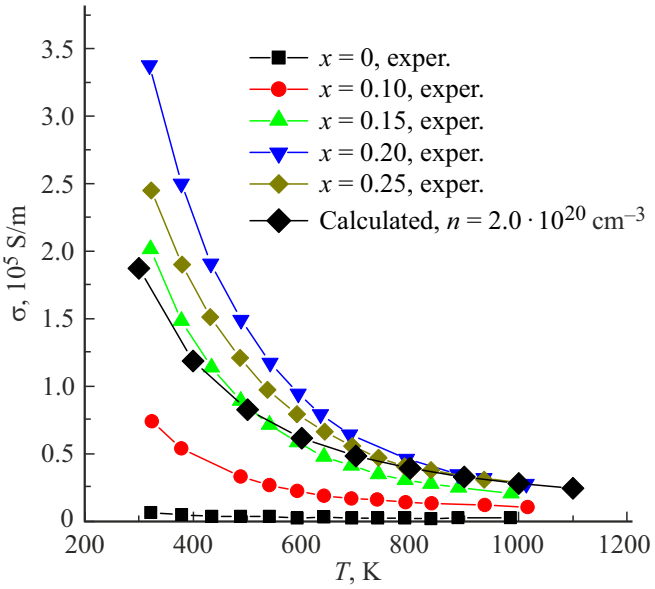

Figure 6. Experimental and calculated data on the conductivity of calcium titanate $Ca_{1-x}La_xTiO_{3-\delta}$ doped with lanthanum and containing vacancies in the oxygen sublattice [27].

ductor character. A similar phenomenon was previously observed in $SrTiO_3$ doped with La at a dopant concentration of $\sim 5\%$ [37], where the semiconductivity was explained by a decrease in the mobility of conduction electrons due to local distortions of the structure near dopant atoms. In our approach, such local distortions are not taken into account. The data on the Seebeck coefficient S shown in Fig. 5 at temperatures up to 500 K correspond well to the experimental data [18] and the results of our previous calculations [36]. The experimentally observed change in the dependence of S on temperature above 500 K correlates with the change in the nature of conductivity at this temperature. In the study [38] in the range of 500–600 K, a change in the size of crystallites and lattice periods by 3% was also observed, i.e. in this case, the deviation of the calculation from the experiment is apparently due to a change in the crystal structure.

In the study [27], experimental data were obtained on TEC of $CaTiO_3$ in the temperature range 300–1000 K. The authors investigated the compounds with vacancies in the oxygen sublattice and estimated the average carrier concentration, $\sim 2.0 \cdot 10^{20}\,cm^{-3}$. Also TECs were studied for a number of lanthanum-doped samples containing oxygen vacancies, and the average carrier concentration was found to be close to $2.0 \cdot 10^{20}\,cm^{-3}$, however, carrier concentrations were not obtained for individual compositions. Fig. 6 shows experimental data [27] on conductivity together with our calculated data at the specified carrier concentration. It can be seen that the calculated data obtained for the average carrier concentration are the average between the conductivity obtained for different compositions.

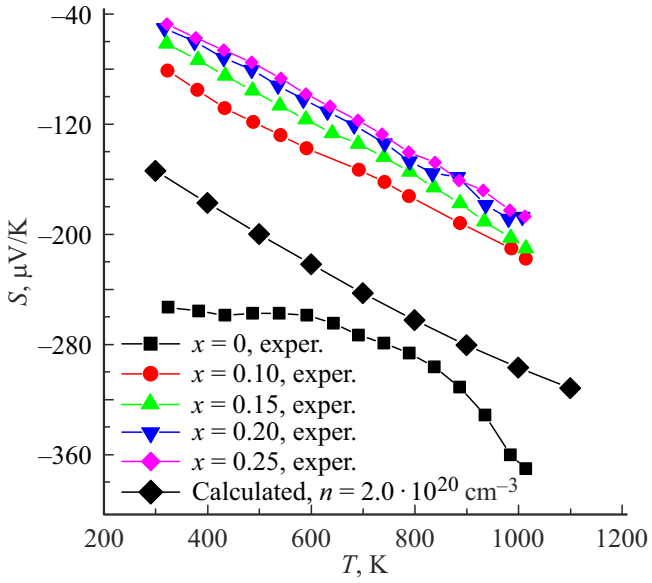

Figure 7. Experimental and calculated data on the Seebeck coefficient for calcium titanate $Ca_{1-x}La_xTiO_{3-\delta}$ doped with lanthanum and containing vacancies in the oxygen sublattice [27].

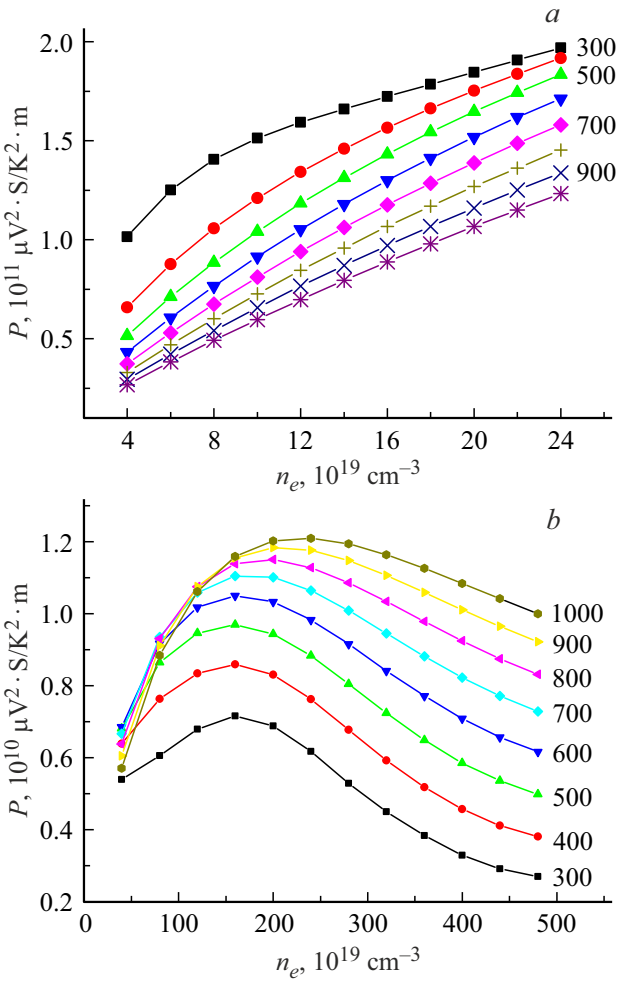

Figure 8. Calculated values of the power function of $SrTiO_3$ for two ranges of carrier concentrations. The temperatures (in kelvins) for which calculations were performed are indicated.

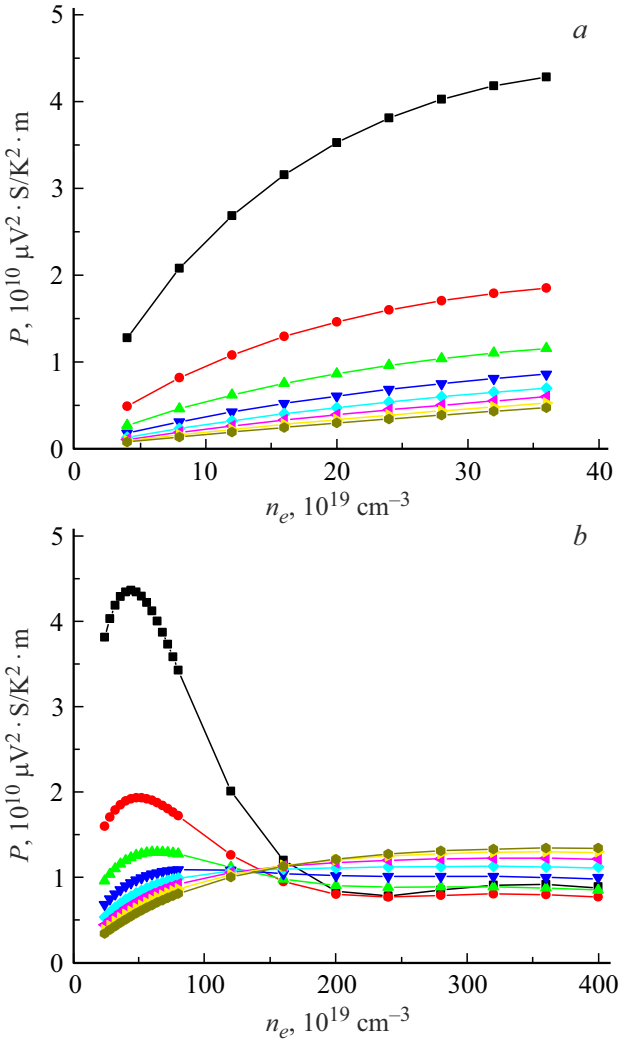

Figure 9. Calculated values of the CaTiO power function$_3$ for two ranges of carrier concentrations. The temperatures correspond to those taken in Fig. 8.

Fig. 7 shows experimental data on the Seebeck coefficient and our calculated data obtained also for the average carrier concentration.

As for conductivity, the calculated data at the average carrier concentration turn out to be the average between the values of the Seebeck coefficient for different compositions. In general, we conclude that when the concentration of doping elements is up to $\sim 5\%$, the method of calculating TEC used by us satisfactorily corresponds to experimental data.

3. Concentration and temperature dependences of the power function

The power function $P = S^2\sigma$, which is included in the numerator of the expression for the ZT value, determines the intensity of the energy flow of carriers in the presence of a temperature gradient, while the thermal conductivity

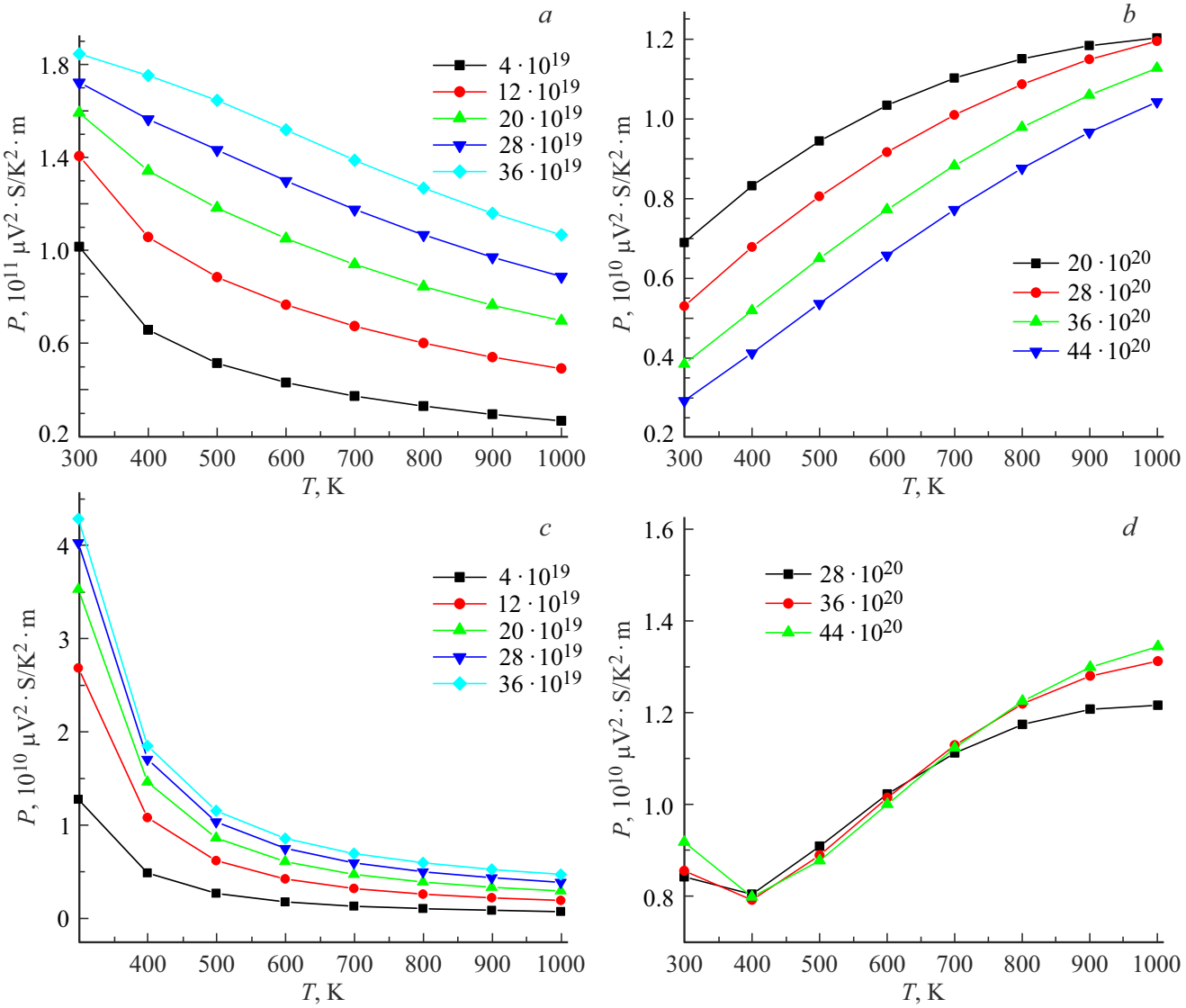

Figure 10. Temperature dependences of the power function at different carrier concentrations. *a, b* — data for $SrTiO_3$, *c, d* — data for $CaTiO_3$.

determines the tendency of the system to equalize the temperature. The standard theoretical approach to evaluating the efficiency of using a thermoelectric material is to calculate the ZT value, which requires calculations of thermal conductivity with large computer resources. Below we will show that less costly calculations of the power function allow us to estimate the optimal concentration of dopants and to qualitatively assess the thermoelectric efficiency of doping compounds.

It follows from Fig. 4–7 that with an increase in the concentration of carriers, the absolute value of the Seebeck coefficient decreases, while the conductivity increases, i.e., the change in the power function with an increase in the concentration of carriers is determined by the balance of two opposite trends. This leads, as calculations show, to the complex nature of the P change, which is shown in Figs. 8, 9.

The values of the power function were calculated for the carrier concentration studied in [18], from 4 to 26. 10^{19} cm^{-3} units, as well as for the range from 40 to 480 10^{19} cm^{-3} units, studied in [15]. In the first case, we observe a decrease of P with an increase in temperature and an increase with an increase in concentration. Obviously, these changes are determined by a change in conductivity, i.e., its decrease due to an increase in the electron-phonon interaction with increasing temperature and an increase due to an increase in the number of conduction electrons. These patterns persist up to a concentration about $100 \cdot 10^{19}$ cm^{-3}, however, at a higher concentration we observe maxima in dependencies, and then a decrease of P, which is associated with a decrease in the value S^2. It follows that the optimal values of the power function can be expected to concentration values ranging from $150 \cdot 10^{19}$ to $250 \cdot 10^{19}$ cm^{-3}, depending on temperature.

We skip the discussion of the results for $BaTiO_3$ since they differ very slightly from the results for $SrTiO_3$. Fig. 9 shows similar graphs for $CaTiO_3$. They also indicate the presence of two ranges in which the dependence of P on concentration has a different character. In the range from 50 to 80 $10^{19}\,cm^{-3}$ units the dependencies have maxima, however, only for temperatures below 600 K, whereas at higher temperatures there are no maxima. We know only one work [5], where the concentration dependence P was explicitly shown, which increases in the range $(10-50)\cdot 10^{19}$ and decreases at concentrations above $120\cdot 10^{19}\,cm^{-3}$. Also the data of works [15,39], in which the temperature and concentration dependences of the power function were obtained, confirm the extreme dependence of P on the carrier concentration in $SrTiO_3$, see Fig. 6 from the specified works. In the review [3], an extreme dependence of the ZT value on temperature for $SrTiO_3$ doped with dysprosium was given, and several similar dependencies for cobaltites with a perovskite structure, which is probably also associated with an extreme change in the power function. However, in most cases, with increasing temperature, the only increases, which is explained by the temperature decrease in thermal conductivity recorded in many works [10–12,15,39]. To obtain specific ZT data, more complex first-principle calculations are required. However, the analysis of the temperature-concentration dependences of the power function shown in Fig. 10 allows us to estimate the range of concentrations promising for obtaining maximum values of ZT at high temperatures.

It follows from the definition of ZT factor (2) that in order to obtain its high values, it is necessary that the decrease in thermal conductivity with an increase in temperature is accompanied by an increase in the power function. As can be seen from Fig. 10, the temperature increase in power function takes place in the second concentration range, whereas in the first range, the power function decreases with increasing temperature, on average 2 times for $SrTiO_3$ and 5 times in $CaTiO_3$. That is, the second range of carrier concentrations, $(200-450)\cdot 10^{19}\,1/cm^3$, is preferable for obtaining high ZT values at high temperatures. For $SrTiO_3$, comparing this estimate with the estimate of the optimal values of the power function depending on the carrier concentration, Fig. 8, we come to the conclusion that in this case the maximum ZT values can be realized at carrier concentrations in the range of $(200-250)\cdot 10^{19}\,1/cm^3$. Qualitatively different conclusions follow for calcium titanate. Here, calculations of the power function show that this value for temperatures of practical interest, above 500 K, in fact does not depend on the concentration of carriers. Therefore, the temperature increase in ZT value known from experiments at a fixed carrier concentration is a consequence of a temperature decrease in thermal conductivity. It follows that for $CaTiO_3$ it is advisable to increase the concentration of dopants, i.e. the concentration of carriers, to the limits determined by the capabilities of the synthesis technology used.

4. Conclusion

Calculations of the thermoelectric characteristics of perovskites $SrTiO_3$, $BaTiO_3$, $CaTiO_3$ indicate that in such compounds, the main mechanism of scattering of electrons in the conduction band generated by doping is the scattering by the Fröhlich mechanism on high-frequency optical phonons. Comparison of the calculated TEC with experimental data indicates a sufficiently high accuracy of calculations, and the observed deviations are apparently associated with distortions of the crystal structure. Calculations of the concentration dependences of the power function at fixed concentrations or temperatures allow us to conclude that the optimal ZT value for $SrTiO_3$ can be achieved in the concentration range $\sim (200-250)\cdot 10^{19}\,1/cm^3$. For $CaTiO_3$, on the contrary, the absence at high temperatures of maxima on the concentration dependences of the power function indicates that the maximum ZT value can be achieved with the maximum possible degree of doping.

The new first-principle approaches developed in recent years to TEC calculations are universal, since they do not use any simplifications related to the type of dispersion of energy bands. Also, no empirical parameters related to the mechanisms of scattering of current carriers are used. Therefore, modeling based on first-principle approaches can serve as a useful means of searching for effective thermoelectrics among compounds with very diverse structures, in particular, as we have shown, to assess the optimal concentrations of doping elements.

Funding

The work was partially supported by St. Petersburg State University (grant No. 90383050). Calculations of the zone structure and TEC were carried out on the URAN cluster of the Institute of Mathematics and Mechanics of the Ural Branch of the Russian Academy of Sciences.

Conflict of interest

The authors declare that they have no conflict of interest.

References

[1] M. Zebarjadi, K. Esfarjani, M.S. Dresselhaus, Z.F. Ren, G. Chen. Energy Environ. Sci. **5**, 5147 (2012).
[2] T. Wu, P. Gao. Materials **11**, 999 (2018).
[3] R. Li, Ch. Zhang, J. Liu, J. Zhou, L. Xu. Mater. Res. Express **6**, 102006 (2019).
[4] M. Yamamoto, H. Ohta, K. Koumoto. Appl. Phys. Lett. **90**, 072101 (2007).
[5] T. Okuda, K. Nakanishi, S. Miyasaka, Y. Tokura. Phys. Rev. B **63**, 113104 (2001).
[6] Sh. Ohta, T. Nomura, H. Ohta, K. Koumoto. J. Appl. Phys. **97**, 034106 (2005).
[7] P. Blennow, A. Hagen, K.K. Hansen, L.R. Wallenberg, M. Mogensen. Solid State Ion. **179**, 2047 (2008).

[8] P. Blennow, A. Hagen, K.K. Hansen, L.R. Wallenberg, M. Mogensen. Solid State Ion. **180**, 63 (2009).
[9] Y. Cui, J.R. Salvador, J. Yang, H. Wang, G. Amov, H. Klaeinke. J. Electron. Mater. **38**, 1002 (2009).
[10] N. Wang, H. Li, Y. Ba, Y. Wang, Ch. Wan, K. Fujinami, K. Koumoto. J. Electron. Mater. **39**, 1777 (2010).
[11] A. Kikuchi, N. Okinaka, T. Akiyama. Scr. Mater. **63**, 407 (2010).
[12] T.T. Khan, I.-H. Kim, S.-Ch. Ur. J. Electron. Mater. **48**, 1864 (2019).
[13] H. Usui, Sh. Shibata, K. Kuroki. Phys. Rev. B **81**, 205121 (2010).
[14] K. Ozdogan, M. Upadhaya Kahaly, S.R. Sarath Kumar, H.N. Alshareef, U. Schwingenschlögl. J. Appl. Phys. **111**, 054313 (2012).
[15] A.V. Kovalevsky, A.A. Yaremchenko, S. Populoh, A. Weidenkaff, J.R. Frade. J. Appl. Phys. **113**, 053704 (2013).
[16] W.S. Choi, H.K. Yoo, H. Ohta. Adv. Funct. Mater., arXiv:1505.02859v1 (2014).
[17] M.U. Kahaly, U. Schwingenschlögl. J. Mater. Chem. A **2**, 10379 (2014).
[18] T.T. Khan, S.Ch. Ur. Electron. Mater. Lett. **14**, 336 (2018).
[19] M.N. Khan, H.-T. Kim, H. Minami, H. Uwe. Mater. Lett. **47**, 95 (2001).
[20] T. Kolodiazhnyi, A. Petric, M. Niewczas, C. Bridges, A. Safa-Sefat, J.E. Greedan. Phys. Rev. B **68**, 085205 (2003).
[21] H. Muta, K. Kurosaki, Sh. Yamanaka. J. Alloys Compd. **368**, 22 (2004).
[22] T. Kolodiazhnyi. Phys. Rev. B **78**, 045107 (2008).
[23] M.B. Smith, K. Page, Th. Siegrist, P.L. Redmond, E.C. Walter, R. Seshadri, L.E. Brus, M.L. Steigerwald. J. Am. Chem. Soc. **130**, 6955 (2008).
[24] S. Lee, G. Yang, R.H.T. Wilke, S. Trolier-McKinstry, C.A. Randall. Phys. Rev. B **79**, 134110 (2009).
[25] T. Bak, J. Nowotny, C.C. Sorreil, M.F. Zhou. Ionics **10**, 334 (2004).
[26] L.H. Oliveira, J. Savioli, A.P. de Moura, I.C. Nogueira, M.S. Li, E. Longo, J.A. Varela, I.L.V. Rosa. J. Alloys Compd. **647**, 265 (2015).
[27] J. Li, Y. Wang, X. Yang, H. Kang, Zh. Cao, X. Jiang, Z. Chen, E. Guo, T. Wang. Chem. Eng. J. **428**, 131121 (2022).
[28] R. Zhang, X. Hu, P. Guo, Ch. Wang. Physica B **407**, 1114 (2012).
[29] A.A. Adewale, A. Chik, R.M. Zaki, F.Ch. Pa, Y.Ch. Keat, N.H. Jamil. Int. J. Nanoelectron. Mater. **12**, 477 (2019).
[30] S. Ponce, E.R. Margine, C. Verdi, F. Giustino. arXiv:1604.03525v2.
[31] J.-J. Zhou, J. Park, I.-T. Lu, I. Maliyov, X. Tong, M. Bernardi. arXiv:2002.02045v1.
[32] A.M. Ganose, J. Park, A. Faghanini, R. Woods-Robinson, K.A. Persson, A. Jain. Naure Commun. **12**, 2222 (2021).
[33] M. Yashima, R. Ali. Solid State Ion. **180**, 120 (2009).
[34] G. Kresse, M. Marsman, J. Furthmuller. Vienna *ab initio* simulation package. VASP the guide. UniversitatWien, Wien (2018). 233 p.
[35] G.D. Mahan. Many-particle physics. Plenum Press, N.Y. (1990). 1032 p.
[36] V.P. Zhukov, E.V. Chulkov. FTT **64**, 418 (2022) (in Russian).
[37] K. Park, J.S. Son, S.I. Woo, K. Shin, M.-W. Oh, S.-D. Park, T. Hyeon. J. Mater. Chem. A, **2**, 4217 (2014).
[38] F. Hanzig, J. Hanzig, E. Mehner, C. Richter, J. Vesely, H. Stocker, B. Abendroth, M. Motylenko, V. Klemm, D. Novikov, D.C. Meyer. J. Appl. Crystallogr. **48**, 393 (2015).
[39] J. Liu, C.L. Wang, H. Peng, W.B. Su, H.C. Wang, J.C. Li, J.L. Zhang, L.M. Mei. J. Electron. Mater. **41**, 3073 (2012).